Academic Journal of Humanities & Social Sciences
ISSN 2616-5783 Vol.3, Issue 2: 124-138, DOI: 10.25236/AJHSS.2020.030214

Optimital Decision-making Model of Mixed Ownership Reform in Power Grid Enterprise for Investing Hrbird Energy System Project

Xiaoxu Fu*, Caixia Tan, Jiang Wang, Jinghan Zhou, Zhongfu Tan

School of Economics and Management, North China Electric Power University, Beijing 102206, China;
**Correspondenc: 183758841@qq.com*

ABSTRACT. *The randomness of wind generation is one of the main factors restricting gird connection of wind generation. The involvements of energy storage systems and resources used for demand response in the process of optimization for wind power are useful means to enhance its regulation capacity. Considering the uncertainty of wind generation in day-ahead plans, this paper proposes a coordinated scheduling optimization model for Wind-ES hybrid systems with demand response via electric vehicles. The model can be used to apply energy storage systems and electric vehicles simultaneously to both peak shaving/valley filling and wind generation plan tracking to achieve the coordination between the on-grid revenue and penalty cost of the hybrid system, so as to develop the optimal strategy for maximum benefits. The wind power is modeled by using scenario analysis method, and the mixed integer programming problem of this paper is solved via CPLEX software. The case study results show that the coordinated scheduling optimization model can not only earn additional revenue for electric vehicle owners, but also effectively improve the economy of wind power grid connection, which provides an important reference for scheduling the demand response resources of electric vehicles to consume wind generation.*

KEYWORDS: *V2G; Wind-ES hybrid systems; scenario reduction; uncertainty; mixed integer programming*

1. Introduction

Due to environmental pollution and fossil resources exhaustion, China has vigorously developed power generation via renewable energy, such as wind. As of the end of 2017, Wind power installed capacity reached 188.82GW, achieving

ISSN 2616-5783 Vol.3, Issue 2: 124-138, DOI: 10.25236/AJHSS.2020.030214

leaping development. However, serious wind curtailment exposed. According to data from the National Bureau of Statistics, the total amount of wind curtailment in 2017 was 41.9 billion , the average annual wind curtailment rate was 11.9% [1], and the amount of wind curtailment was over 10% for three consecutive years.

The energy storage system with large capacity has the ability of rapid two-way regulation. It is an effective way to alleviate wind curtailment in wind power plants where energy storage devices are employed. There have been relevant researches on the wind-ES hybrid system operation for wind curtailment reduction. Reference [2] constructed a multi-time wind-ES joint dispatch model, chasing the maximum expected income, and the randomness of wind generation is simulated by using scenario reduction technology in the paper. Reference [3] considered the risk of load loss in the meantime of purchasing the maximum revenue of the wind-ES hybrid system, and constructed a multi-objective scheduling model for the hybrid system operation. Reference [4] constructed a two-stage stochastic optimization model considering the influences of wind power forecast error and uncertainty of electricity price on the system benefits. Reference [5] proposed an intraday rolling coordinated dispatching mode and a two-stage optimization model, based on ultra-short-term output forecast of wind power plants, which is conducive to benefit increase, as well as wind curtailment reduction and operation cost reduction. Reference [6] constructed a cooperated optimization model and applied it to alleviating wind curtailment and providing grid secondary frequency modulation service, and the conclusion was drawn that energy storage for dispatching can reduce wind curtailment in wind-power-restricted periods, and increase the income from on-grid operation via frequency modulation when wind power generation is free. Reference [7], considering the applications of energy storage systems to two modes of peak regulation and plan tracking, conducted a multi-mode coordination optimization.

The above literature mainly studied how power generation side promoted wind power consumption via energy storage systems. However, it is not enough for large-scale grid to alleviate fluctuation of wind power output only via energy storage [8-9]. Research on coordinated dispatch of wind-ES hybrid systems with demand response (DR) is conducive to further enhance the wind power consumption ability of power systems. Reference [10] considered price elasticity matrix to encourage user side to participate in peak regulation, and constructed a wind-thermal-ES coordinated dispatching model with DR, which is capable of effectively increase the wind power consumption, in the meantime of decreasing coal consumption. However, the mentioned model only sketched DR and the constraints were simple. References [11-12] concretely modeled price-based demand response (PBDR) and incentive-based demand response (IBDR), and conducted multi-demand-response stochastic optimization with the conclusion that mixed consideration of DR and energy storage had better economic benefits and greater wind power consumption.

Electric vehicles, as a vital load resource, are seen as a distributed ES unit via “vehicle to grid” (V2G), interacting with generation side, to consume surplus wind power. Reference [13] proposed a wind-electric vehicle coordinated dispatching model in different gird connection modes of electric vehicle, and applied the improved constraint methods and fuzzy decision theories for model solving; yet the

ISSN 2616-5783 Vol.3, Issue 2: 124-138, DOI: 10.25236/AJHSS.2020.030214

price's influence on the proposed model was not involved. Reference [14] used the time-of-use price to encourage users to orderly charge/discharge electric vehicles, and NSGA-II is employed for model solving; The results indicated that the orderly grid connection of electric vehicles can effectively narrow the peak-valley difference of load and the operating cost of thermal generation, but wind power uncertainty is absent in the paper.

Under the above background, aiming at the maximum expected revenue of the wind-ES hybrid system, this paper establishes a day-ahead optimization model with electric vehicles (as DR resources) included. The limited output scenario generated by Monte Carlo simulation and scenario reduction is applied to simulating the wind generation uncertainty. CPLEX software is employed since the proposed model is a mixed integer programming (MIP) problem. Based on the case study results, the coordinated operation revenue of the wind-ES hybrid system under different modes is analyzed, and discusses the influence of the peak-valley price difference and the deviation penalty coefficient on the revenue of the hybrid system.

2. Wind power prediction model based on scenario analysis

The scenario analysis is a method that decomposes the uncertain stochastic process into typical scenarios with discrete probability, and the wind generation uncertainty through the set of determined probability scenarios is described. Its main content includes scenario generation and scenario reduction. The steps of simulating wind power output by using scenario analysis method are as follows:

(1) According to the auto regression moving average (ARMA), the wind speed is predicted.

(2) Latin hypercube stratified sampling is applied to sampling the wind speed prediction error, and the probability of each sample is assumed to be equal.

(3) Backward reduction technology is used to reduce the sample set of prediction error scenarios and merge similar scenarios.

(4) According to the relationship between wind speed and output, the wind power limited output scenario and the corresponding scenario's probability are determined.

2.1 Wind speed prediction model considering prediction error

The ARMA model can minimize the variance to predict the wind speed [15]. Based on the wind farms' historical data, wind speed prediction error is simulated via ARMA (1,1).

Wind speed over time t is set to be $g_{w,t}$, which is calculated as follow.

$$g_w(t) = g_w^f(t) + \Delta g(t) \tag{1}$$

ISSN 2616-5783 Vol.3, Issue 2: 124-138, DOI: 10.25236/AJHSS.2020.030214

Where $g_w(t)$ stands for wind velocity, $g_w^f(t)$ is the predicted wind velocity, and $\Delta g(t)$ is the predicted error of wind speed over time t.

The predicted error of wind speed model is calculated as follow.

$$\Delta g(t) = \varphi \cdot \Delta g(t-1) + Z(t) + \tau \cdot Z(t-1) \quad (2)$$

Where $\Delta g(t-1)$ indicates the predicted wind velocity error over time $t-1$, $Z(t)$ is the random variable that obeys $N(0,\ \sigma^2)$, φ stands for the autoregressive parameter, and τ stands for the sliding average parameter (both of which can be obtained via the minimum ARMA and mean square error of wind speed from historical data).

2.2 Wind speed prediction error scenario generation based on Latin hypercube sampling

The principle of using many scenarios to simulate wind speed error is to concretize the wind speed uncertainty via a random number subject to a certain distribution, and then obtain the wind output model. Based on the wind speed prediction model in Section 1.1, this section samples the wind speed error, via Latin hypercube sampling, in order to obtain the scenario set of wind speed prediction error. The schematic diagram of Latin hypercube sampling is shown in Fig. 1.

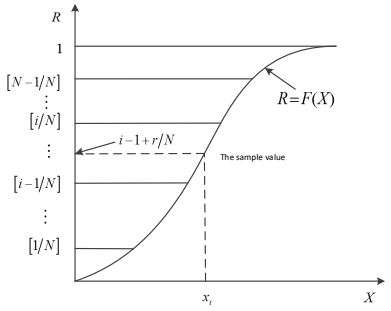

Fig. 1. Latin hypercube sampling schematic diagram

The steps of wind speed sampling with Latin hypercube sampling technology are as follows [16].

(1) The probability density function of wind speed prediction error is divided into equal probability intervals, that is, $[0,1/N],[1/N,2/N],[N-1/N,1]$;

(2) in respect to $[i-1/N,i/N]$, $1 \le i \le N$ (any probability interval), select a number randomly and take it as p_i:

ISSN 2616-5783 Vol.3, Issue 2: 124-138, DOI: 10.25236/AJHSS.2020.030214

$$p_i = \frac{r}{N} + \frac{i-1}{N} \tag{3}$$

Where r stands for a random value which is between 0 and 1;

(3) The sample value of wind speed prediction error, which is in the probability interval $[i-1/N, i/N]$, is obtained via the inverse function $F^{-1}(R)$, i.e. $x_i = F^{-1}(R_i)$.

Through the above steps, the random variables of wind speed prediction can be obtained. In order to reduce the correlation of the sample data in the sampling matrix and get the independent sampling matrix, Cholesky decomposition method is used to sort the sampling matrix. The steps are detailed in [17].

2.3 Wind speed scenario reduction

It is of necessity to merge/remove similar scenarios in the same set to improve the accuracy and efficiency of calculation, and then obtain a representative set that has enough samples to describe a random predicted distribution of wind speed, so that the typical scenario set after reduction can still represent the initial set when it comes to probability.

(1) Assuming that the wind speed prediction error sample, i.e. the number of initial scenarios is set to be N, and the number of terminal scenarios is set to be n. The probability of each initial scenario is detailed as follows.

$$p_i = \frac{1}{N} \tag{4}$$

The number of scenarios when iterating is set to be n', $n' = N$ when initializing.

(2) For any two scenarios in the n' in the iteration process, the Kantorovich distance between the two scenarios is calculated by taking the 24-hour wind speed prediction error scenario vector as the reduction unit, which is simplified as an absolute value, i.e.

$$d_k(u_i, u_j) = \left| u_i - u_j \right| \tag{5}$$

(3) The wind speed prediction error scenario u_j closest to its scenario is calculated, i.e. $d_k(u_i, u_j) = \left| u_i - u_j \right|$; also, the probability distance between the two scenarios is calculated, i.e.

$$P_{DKi} = \min\left\{ d_k(u_i, u_j) i \neq j \right\} \times p_i \tag{6}$$

ISSN 2616-5783 Vol.3, Issue 2: 124-138, DOI: 10.25236/AJHSS.2020.030214

(4) Repeat step 3, and the minimum scenario distance is calculated, which is taken as P_{DKS}, in respect to each wind speed prediction error scenario.

$$P_{DKS} = \min\left\{P_{DKi} \mid 1 \le i \le n'\right\} \tag{7}$$

(5) Update the scenario probability, i.e. $p_i = p_i + p_j$, and remove the u_j from the wind speed prediction error set.

(6) Update the scenario set number, i.e. $n' = n' - I$, in the scenario iteration where I is the scenario number that has been removed. Then repeat steps 2-5 until the scenarios are reduced to n which is target number.

(7) The wind speed prediction error in each scenario is superposed with the wind speed basis, and the multi-scenario model of wind speed prediction is given.

2.4 Wind power output model construction

On the basis of the reduced wind speed prediction scenario in section 1.3, the wind output is calculated according to wind speed, and the wind output model is non-linear. To simplify the analysis, this paper assumes that the wind output is not affected by interaction between fans but wind speed. The fan output characteristic curve is given in [18], and the approximate output formula is given as follows.

$$P_t^w = \begin{cases} 0 & g_w(t) \le g_{in} \\ a_1 + a_2 g_w^3(t) + a_3 g_w^2(t) + a_4 g_w(t) & g_{in} \le g_w(t) < g_{out} \\ P_N & g_w(t) \ge g_{out} \end{cases} \tag{8}$$

Where $P_{PV}(t)$ is the wind output, P_N is the rated output, a_1, a_2, a_3, a_4 are all the fitting coefficients, g_{in} is the minimum wind speed when it outputs, and g_{out} is the minimum wind speed when the fan operates in rated power.

By using formula (8) and the wind speed prediction scenario generated after reduction, the wind power prediction output curve of the corresponding specified number of scenarios can be obtained.

3. Wind-ES coordinated scheduling optimization model construction

3.1 Objective function

Based on the output scenario simulation of different wind farms and the charging/discharging power prediction curves of electric vehicles, the coordinated scheduling model is constructed for wind-ES hybrid system with electric vehicles, chasing the objective of the maximum expected revenue of the system in different wind speed scenarios, which is shown in formula (9). In this model, energy storage

ISSN 2616-5783 Vol.3, Issue 2: 124-138, DOI: 10.25236/AJHSS.2020.030214

system and electric vehicles play two roles: peak regulation and tracking planned output. When it is applied to peak regulation, energy storage system and electric vehicles release energy in peak periods to gain revenue, which is charged in valley periods. When it is applied to tracking planned output, the system chases the minimum penalty cost, and the planned/actual output deviation is narrowed by controlling energy storage.

$$f = \max E\left[\sum_{\omega=1}^{N_s}\rho^{\omega}\sum_{t=1}^{T}\left[\pi_t\left(P_t^{\omega,w}+P_t^{\omega,dis}-P_t^{\omega,ch}\right)\Delta t - C_t^{\omega,pun} - C_t^{\omega,DR}\right]\right] \quad (9)$$

Where ω stands for the wind power scenario, N_s stands for the number of wind power farm, ρ^{ω} stands for the probability of ω, t stands for the time series where 1h is seen as a period, T stands for the total periods within a day, π_t stands for the price of the wind-ES hybrid system in grid-connected operation over time t, $P_t^{\omega,w}$ is the output of wind power farm in scenario ω over time t, $P_t^{\omega,dis}$ and $P_t^{\omega,ch}$ are respectively the discharging/charging power in scenario ω, Δt is the calculating duration, $C_t^{\omega,pun}$ is the penalty cost in scenario ω over time t, and $C_t^{\omega,DR}$ is the DR cost of electric vehicles over time t.

When an electric vehicle participates in the coordinated operation of the hybrid system, its DR cost is expressed as follows.

$$C_t^{\omega,DR} = \pi_t^{ev}\sum_{t=1}^{T}\left|\sum_{g=1}^{G}P_t^{\omega,g}\right| \quad (10)$$

Where π_t^{ev} is the price of electric vehicles providing ancillary service in day-ahead market over time t, $P_t^{\omega,g}$ is the charging/discharging power of vehicle g over time t, G is the number of electric vehicles.

3.2 Constraints

The constraints of day-ahead scheduling include penalty cost constraints, wind farm output constraint, day-ahead wind capacity planning constraint and energy storage battery constraints.

(1) Penalty cost constraint

The penalty cost is expressed by the linear constraint in [19], as shown in Fig. 2 where P_t^{plan} refers to the day-ahead generation plan submitted by the hybrid system to the grid, and μ_t^{up} and μ_t^{down} are respectively the penalty prices at time t when the output exceeds the upper limit or is lower than the lower limit, and ΔP^{dev} indicates the deviation between the allowable wind farm output plan and the actual value.

ISSN 2616-5783 Vol.3, Issue 2: 124-138, DOI: 10.25236/AJHSS.2020.030214

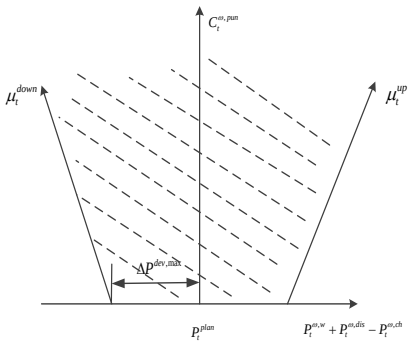

Fig. 2. The schematic of penalty cost

The minimum in the shadow area of the figure indicates the penalty cost, which is detailed as follows.

$$\begin{cases} C_t^{\omega,pun} \geq \mu_t^{up}\left(P_t^{\omega,w}+P_t^{\omega,dis}-P_t^{\omega,ch}-P_t^{plan}+\sum_{g=1}^{G}P_t^{\omega,g}-\Delta P^{dev}\right)\Delta t \\ C_t^{\omega,pun} \geq \mu_t^{down}\left(P_t^{plan}-\Delta P^{dev}-P_t^{\omega,w}-P_t^{\omega,dis}+P_t^{\omega,ch}-\sum_{g=1}^{G}P_t^{\omega,g}\right)\Delta t \\ C_t^{\omega,pun} \geq 0 \end{cases} \tag{11}$$

Considering power grid security, the deviation between the actual output and the planned value is limited by the maximum value $\Delta P^{dev,\max}$.

$$-\Delta P^{dev,\max} \leq P_t^{plan}-P_t^{\omega,w}-P_t^{\omega,dis}+P_t^{\omega,ch}-\sum_{g=1}^{G}P_t^{\omega,g} \leq \Delta P^{dev,\max} \tag{12}$$

(2) Wind farm output constraint

$$0 \leq P_t^{\omega,w} \leq P_t^{\omega,w,\max} \tag{13}$$

Where $P_t^{\omega,w,\max}$ is the predicted wind output in scenario ω over time t.

(3) Day-ahead wind capacity planning constraint

$$0 \leq P_t^{plan} \leq P_{dis}^{\max}+P_w^{\max} \tag{14}$$

Where $P_{dis}^{\max}$ is the maximum discharging output of energy storage battery, and $P_w^{\max}$ is the maximum wind output.

(4) Energy storage battery constraints

Energy storage battery operation constraints include battery capacity constraint,

ISSN 2616-5783 Vol.3, Issue 2: 124-138, DOI: 10.25236/AJHSS.2020.030214

capacity constraint, energy balance constraint at the beginning and end of the energy storage cycle, charging and discharging power constraints, and battery state transition constraints [20].

$$\begin{cases} E_{t+1}^{\omega} = E_t^{\omega} + P_t^{\omega,ch}\Delta t\eta_{ch} - P_t^{\omega,dis}\Delta t / \eta_{dis} \\ E^{\min} \le E_t^{\omega} \le E^{\max} \\ E_0^{\omega} = E_T^{\omega} \\ 0 \le P_t^{\omega,ch} \le P_{ch}^{\max} U_t^{\omega,ch} \\ 0 \le P_t^{\omega,dis} \le P_{dis}^{\max} U_t^{\omega,dis} \\ U_t^{\omega,ch} + U_t^{\omega,dis} = 1 \end{cases} \tag{15}$$

Where E_t^{ω} is the electric quantity of the battery in scenario ω during time t, η_{ch} and η_{dis} are respectively the charging/discharging efficiency, $E^{\max}$ and $E^{\min}$ are the limitations of the battery, E_0^{ω} and E_T^{ω} are respectively the initial and terminal states in scenario ω, $U_t^{\omega,ch}$ and $U_t^{\omega,dis}$ are respectively the charging and discharging variables of the battery in scenario ω during time t, therein 0 stands for "off" while 1 stands for "on".

(5) State transformation of energy storage battery constraint

To avoid the frequent charge/discharge state change and improve the life of energy storage battery, it is necessary to limit the charge/discharge state frequency as follows.

$$\sum_{t=1}^{T} Y_t^{\omega,bat} \le N_{bat} \tag{16}$$

$$Y_t^{bat} = \left| U_t^{\omega,dis} - U_{t-1}^{\omega,dis} \right| \tag{17}$$

Where $Y_t^{\omega,bat}$ is the state transformation variable in scenario ω, and N_{bat} is the frequency limitation of charging/discharging of the battery.

3.3 Case study

(1) Basic data

It is assumed that a wind farm consists of 200 fans, and all fans are exposed in the same environment at the same time. The autoregressive parameter φ and sliding average parameter τ in the wind speed prediction error model are respectively 0.78 and -0.34, and σ is set to be 1. The wind speed are set based on the wind speed data of a wind farm (every 10min a day), the rated output of a single fan is 3MW, and wind speed and wind output curve refer to [21].

ISSN 2616-5783 Vol.3, Issue 2: 124-138, DOI: 10.25236/AJHSS.2020.030214

The allowable maximum wind output deviation is 50% of the rated capacity of the wind farm. The capacity of energy storage battery is 50MW, the maximum charge and discharge power is 10MW, the charge/discharge efficiency is 90%, and the energy storage battery states at 20% ~ 100%.

One thousand scenarios are generated by Monte Carlo simulation technology, and 10 scenarios are final-chosen via fast backward method [22].

Time-of-use price is used for the wind-ES system connected to grid, which is 750 yuan/MW in peak periods (11:00-15:00 and 19:00-21:00), 500 yuan/MW in flat periods (08:00-10:00, 16:00-18:00 and 22:00-23:00), and 250 yuan/MW in valley period (0:00-7:00). The penalty price is 1.1 times of the grid-connected electricity price.

Assuming that 20 thousand electric vehicles participate in the coordinated scheduling, the orderly charging and discharging power curves of electric vehicles are shown in Fig. 3 [23].

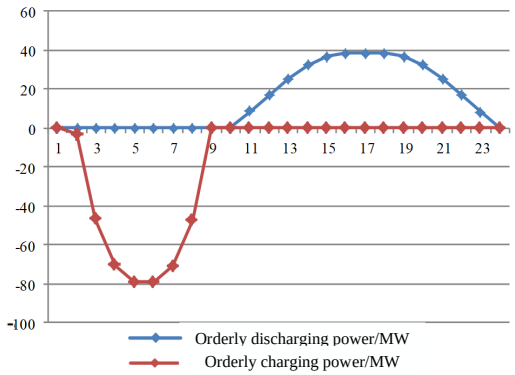

Fig. 3. Electric vehicle orderly charging and discharging curves

(2) Influences of electric vehicles on scheduling results

Set the coordinated scheduling of electric vehicles participating in the wind-ES hybrid system as mode 1 and not participating in the coordinated scheduling as mode 2. The operation results in different modes are shown in Table 1.

Table 1. The results under different modes

Mode	Expected grid-connected revenue/10^4 yuan	Expected penalty cost/10^4 yuan	Expected revenue from electric vehicles/10^4 yuan	Expected coordinated operation revenue /10^4 yuan
Mode 1	154.03	34.88	4.81	114.34
Mode 2	150.76	42.34	—	108.42

Comparing the results in the table, the participation of electric vehicles in the

ISSN 2616-5783 Vol.3, Issue 2: 124-138, DOI: 10.25236/AJHSS.2020.030214

coordinated operation has better economic benefits. On the one hand, electric vehicles involved in the coordinated operation is charged with the surplus wind power and discharged when insufficient wind output happens, which plays the role in peak shaving and valley filling, and improves the grid-connection income of the hybrid system. On the other hand, electric vehicles participating in the coordinated operation of the hybrid system makes the wind farm have greater regulation capacity, so that the penalty cost of wind farm due to the wind generation uncertainty is greatly reduced. In addition, the participation of electric vehicles in the coordinated operation can obtain ancillary service costs, reduce charging costs, and improve the initiative of electric vehicle owners to participate in grid dispatching.

(3) Influences of different time-of-use prices on the calculation results

The penalty fee is set to be 1.1 times of the grid-connected price, and the price in flat periods is 500 yuan/MW. The prices in peak and valley periods are 50% - 70% higher than that in flat periods. The results of electric vehicles participating in the coordinated operation are shown in Figs. 4-5.

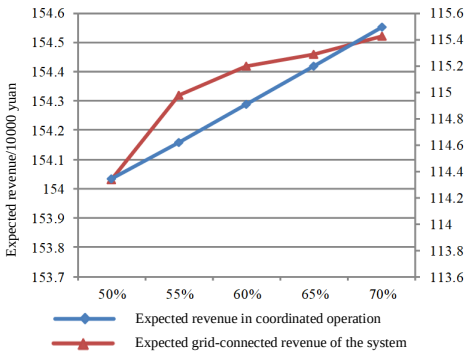

Fig. 4. Expected grid-connected revenue of the system and expected revenue in coordinated operation

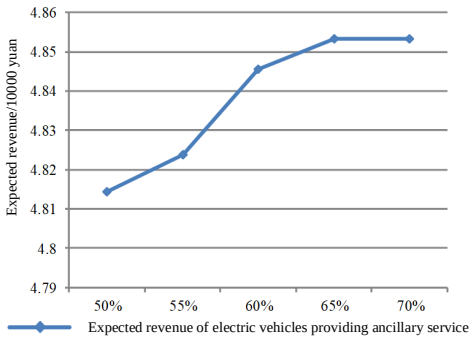

Fig. 5. Expected revenue of electric vehicle providing ancillary service

ISSN 2616-5783 Vol.3, Issue 2: 124-138, DOI: 10.25236/AJHSS.2020.030214

It can be seen from the figure that the greater the price difference between time-of-use prices, the higher the expected revenue from grid-connection and the expected revenue in coordinated operation. The greater the price difference between time-of-use prices, the more surplus wind power is absorbed by electric vehicles and energy storage system in valley periods, and the higher the revenue obtained by releasing the surplus wind power in peak periods.

(4) Influence of different penalty coefficients on the results

The peak-valley price difference is taken as 50%, and the operation results of mode 1 and mode 2 with different penalty coefficients are shown in the figures. Figs. 6-7 respectively show the expected grid-connected revenue of the system and the expected penalty costs.

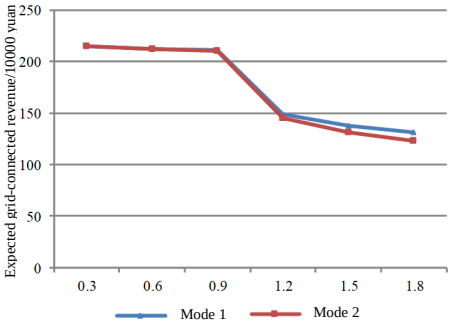

Fig. 6. Expected grid connected revenue under different penalty coefficients

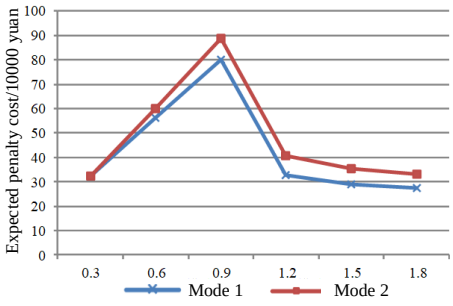

Fig. 7. Expected penalty cost under different penalty coefficients

The penalty coefficients reflect the controllability requirements of the grid for wind power grid connection. When the penalty coefficient is less than 1, the wind power has the priority of scheduling, but the equivalent revenue of the limitation crossing part will be reduced. When the penalty coefficient is greater than 1, the

ISSN 2616-5783 Vol.3, Issue 2: 124-138, DOI: 10.25236/AJHSS.2020.030214

extra power will generate penalty. According to Figs. 6-7, when the penalty coefficient is less than 1, the expected revenue of the hybrid system is basically the same under different penalty coefficients. Even if the penalty cost increases with the increase of the penalty coefficient, the penalty cost will not be reduced by reducing the wind power generation. When the penalty coefficient is greater than 1, the penalty cost is greater than the revenue from grid connection. The wind-ES hybrid system reduces the penalty cost by reducing the power that gets access to public grid.

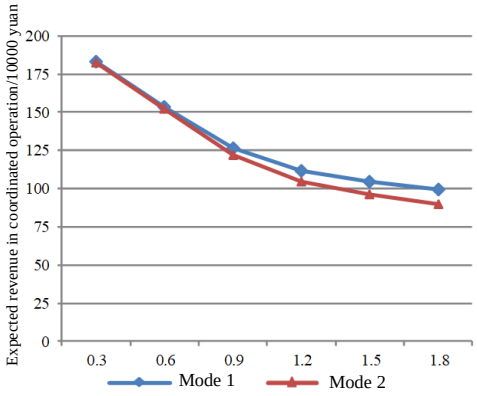

Fig. 8. Expected revenue in different modes under different penalty coefficients

The net expected revenue of mode 1 and mode 2 under different penalty coefficients are shown in Fig. 8. It can be seen from the figure that for different penalty coefficients, the expected revenue in coordinated operation in mode 1 is higher than that in mode 2. The main reason is that in mode 1, electric vehicles participating in the coordinated operation makes them have greater price handling ability to cope with the wind power fluctuation and reduce the penalty cost.

4. Conclusions

Based on different wind power predicting scenarios, a day-ahead scheduling model for wind-ES hybrid systems with electric vehicles, considering the uncertainty of wind power output, is proposed. Through a case study the benefits of electric vehicles participating in the operation of the wind-ES hybrid system are verified and compared, and the influences of the price factors on the operation results are discussed. This paper concludes as follows.

(1) Electric vehicles, as DR resources, are employed in wind-ES hybrid systems, which are conducive to making the wind farm have more scheduling flexibility, effectively improve the economy of wind power getting access to grid, and promote the wind power consumption.

ISSN 2616-5783 Vol.3, Issue 2: 124-138, DOI: 10.25236/AJHSS.2020.030214

(2) The participation of electric vehicles in the operation of the wind-ES hybrid system can improve the regulation capacity of the wind farm, which is ultimately reflected in two aspects that are the grid-connected revenue via peak regulation and the penalty cost reduction via tracking planned output. Different price factors have a great influence on the revenue of the wind-ES hybrid system. Therefore, it is necessary to develop appropriate time-of-use price mechanism and deviation assessment mechanism to better promote the consumption of wind power for grid connection.

References

[1] Wind power grid connected operation of NEA in 2017 [EB / OL]. [2018-1-26.]
[2] Wu Xiong, Wang Xiuli, Li Jun, et al. Joint scheduling model and solution of wind energy storage hybrid system [J]. Chinese Journal of electrical engineering, 2013,33 (13): 10-17.
[3] Dukpa A, Duggal I, Venkatesh B, et al. Optimal participation and risk mitigation of wind generators in an electricity market[J]. IET Renewable Power Generation, 2010, 4(2): 165-175.
[4] Garcia-Gonzalez J, De l M R M R, Santos L M, et al. Stochastic joint optimization of wind generation and pumped-storage units in an electricity market[J]. IEEE Transactions on Power Systems, 2008, 23(2): 460-468.
[5] Huang Yang, Hu Wei, min Yong, Luo Weihua, Wang Zhiming, Ge Weichun. Multi objective coordinated scheduling of wind storage joint system considering day ahead planning [J]. Chinese Journal of electrical engineering, 2014,34 (28): 4743-4751.
[6] Hu Zechun, Xia Rui, Wu Linlin, Liu Hui. Optimization strategy of wind storage combined operation considering energy storage participating in frequency modulation [J]. Grid technology, 2016,40 (08): 2251-2257.
[7] Lu Qiuyu, Hu Wei, min Yong, Wang Zhiming, Luo Weihua, Cheng Tao. Multi mode coordination and optimization strategy of wind storage system considering time dependence [J]. Power system automation, 2015,39 (02): 6-12.
[8] You Yi, Liu Dong, Zhong Qing, et al. Multi objective optimization of energy storage system in active distribution network [J]. Power system automation, 2014, 38 (18): 46-52.
[9] He Chuan, Liu Tianqi, Hu Xiaotong, Li Xi, Li Xingyuan. Optimal control of wind power climbing based on ultra short term wind power prediction and hybrid energy storage [J]. Grid technology, 2017,41 (03): 782-790.
[10] Song Yihang, Tan Zhongfu, Li Huanhuan, et al. Joint optimization model of generation side, storage side and demand side to promote wind power consumption [J]. Grid technology, 2014, 38 (3): 610-615.
[11] Ju Liwei, Qin Chao, Wu Hongliang, et al. Stochastic optimization scheduling model of wind power consumption considering multi type demand response [J]. Grid technology, 2015, 39 (7): 1839-1846.
[12] Xu Hui, Jiao Yang, Pu Lei, Tan Zhongfu, et al. Stochastic scheduling optimization model of integrated virtual power plant with wind and gas storage considering uncertainty and demand response [J]. 2017, 41 (11): 3590-3597.

ISSN 2616-5783 Vol.3, Issue 2: 124-138, DOI: 10.25236/AJHSS.2020.030214

[13] Ju Liwei, Li Huanhuan, Chen Zhihong, et al. Comparative analysis model of wind power electric vehicle multiple grid connection modes based on two-step adaptive algorithm [J]. Grid technology, 2014, 38 (6): 1492-1498.
[14] Hou Jianchao, Hu Qunfeng, Tan Zhongfu. Multi objective optimization model of wind power electric vehicle coordinated dispatching considering demand response [J]. Electric power automation equipment, 2016, 36 (7): 22-27.
[15] Pan DIF, Liu Hui, Li Yanfei. Improved algorithm for short-term multi-step prediction of wind speed in wind farms [J]. Chinese Journal of electrical engineering, 2008, 28 (26): 87-91.
[16] Deng Yong. Research on optimal scheduling of power system units with wind farms [D]. Chongqing University, 2014.
[17] Yan Zhengang. Study on micro grid economic dispatch considering the randomness of micro sources [D]. Southwest Jiaotong University, 2017.
[18] Matevosyan J, Soder L. Minimization of imbalance cost trading wind power on the short-term power market[J]. IEEE Transactions on Power Systems, 2006, 21(3):1396-1404.
[19] Dai Yuanhang, Chen Lei, min Yong, Xu Fei, Hou Kaiyuan, Zhou Ying. Optimal operation of wind farm and cogeneration with heat storage [J] Chinese Journal of electrical engineering, 2017,37 (12): 3470-3479 + 3675.
[20] Xie Yingzhao, Lu Jiping. Multi objective unit combination optimization model and solution of wind storage hybrid system ［J］. Electric power automation equipment, 2015, 35 (3): 18-26.
[21] Matevosyan, Julija, Söder, Lennart. Minimization of imbalance cost trading wind power on the short-term power market[J]. IEEE Transactions on Power Systems, 2006, 21(3):1396-1404.
[22] Holger Heitsch, Werner Römisch. Scenario Reduction Algorithms in Stochastic Programming[J].Computational Optimization and Applications, 2003, 24(2-3):187-206.
[23] Shi Quansheng, Ping zongfei, Chen Minjun. Price linkage model considering electric vehicle access [J]. Electric power automation equipment, 2014,34 (11): 34-40.